





Monitoring of Land Subsidence using PSInSAR: A Case Study in Nanjing Urban Area

Miao Hou¹^a, Yongping Xu²^b, Huaiqian Xiao², Houjun Yan², Xing Yang¹^{c*}
and Songgan Weng¹^d

¹Jiangsu Hydraulic Research Institute, 97 Nanhu Road, Nanjing 210017, China

²Jiangsu Administration of Huaihe, Shuhe and Xinhe Rivers, 8 Shenzhen Road, Huaian 223005, China

Keywords: Land subsidence, Nanjing, PSInSAR, Sentinel-1, Urban area


Abstract: Urban land subsidence is mainly induced by human activities, such as ground-water overdraft, mining of mineral resources and load of constructions. The geodetic-based monitoring systems utilizing leveling have been used to study land subsidence in many urban subsidence regions for a long time. But many benchmarks established for leveling have been destroyed or are unstable due to human activities or land subsidence. In addition, conventional leveling in urban areas is costly and time-consuming, often taking months or years to complete land subsidence measurement. So, it is of great significance to adopt new measurement technology in urban land subsidence monitoring. Nanjing city with rapid urbanization, a large city in China, has suffered subsidence problems in the past 30 years. This paper uses the Permanent Scatterers Synthetic Aperture Radar Interferometry (PSInSAR) methodology with Synthetic Aperture Radar (SAR) images acquired from the Sentinel-1 between 2014 and 2019 to characterize the subsidence of Nanjing city, which provides high-resolution assessment of deformations for sluices, bridges, high-rise buildings, historical buildings and so on. The analysis shows that PSInSAR is very efficient space-borne technique for monitoring subsidence phenomena in urban area.


1 INTRODUCTION


As a global disastrous natural hazard, land subsidence may occur in large urban areas over the world and usually caused by human activities, such as ground-water overdraft, mining of mineral resources and load of constructions. However, the conventional geodetic technique utilizing leveling is costly and time-consuming in the large-scale urban land subsidence monitoring. Interferometric synthetic-aperture radar (InSAR) is a modern space-borne technology for monitoring earth surface deformation. InSAR techniques (e.g. DInSAR, PSInSAR, SqueeSAR) can provide centimeter- to millimeter-level accuracy in large-scale land subsidence monitoring without much time and high cost. Also, InSAR techniques have the advantages of all-weather adaptability (Yu et al., 2021; Yang et al.,


2020; Alani et al., 2020). InSAR techniques have been successfully applied in different deformation research work, such as glacier drift (Yan et al., 2016), surface subsidence (zhou et al., 2020; Smith & Knight, 2019), landslide (Guo et al., 2021; Fobert et al., 2021), volcanic eruption (Liang et al., 2021; Hooper, 2008), etc.

Wright et al. (2004) used InSAR to measure surface displacement across the western Tibetan plateau. Pritchard & Simons (2013) used InSAR to analyze the deformations of 900 remote volcanos in the central Andes to determine which one might have magma moving at depth. Baer et al. (2002) used 16 SAR images obtained by the European Remote Sensing ERS-1 and ERS-2 satellites from 1992 to 1999 to research land subsidence along the Dead Sea shores. Rivera et al. (2017) used COSMO-SkyMed InSAR to obtain time-dependent ground deformation

^a <https://orcid.org/0000-0002-0924-615X>

^b <https://orcid.org/0000-0002-2583-8534>

^c <https://orcid.org/0000-0002-5512-1817>

^d <https://orcid.org/0000-0003-2122-8576>

data over Cotopaxi volcano. Koning et al. (2020) carried out the land subsidence monitoring using InSAR in a dike strengthening project and obtained the land subsidence rate. Xu et al. (2018) reviewed the applications of remote sensing technology, such as InSAR, in urban flood simulation.

Nanjing city with rapid urbanization, a large city in China, had suffered serious subsidence problems in the past 30 years. Geological hazards caused by land subsidence, such as the building tilt, ground collapse and embankment deformations, have long been a problem affecting the development of Nanjing and resulted in increased flood risk in some urban subsidence regions, especially in Hexi area of Nanjing city, where the soft soil layer is widely distributed. Therefore, urban land subsidence monitoring in Nanjing is of great significance. This paper takes Nanjing as an example, and four types of buildings (i.e. sluice, bridge, historic building and high-rise building) are selected as research cases to carry out the application research of InSAR technology in urban land subsidence monitoring. This paper is structured as follows: At first, the research background is presented in Section 1. Then, the study area and InSAR data is introduced in Section 2. Section 3 presents the InSAR method. And, the results are summarized in Section 4. Finally, main conclusions are presented in Sections 5.

2 STUDY AREA AND DATA

Nanjing city, the capital of Jiangsu Province, is located in the lower reaches of the Yangtze River and in the southwest of Jiangsu Province (Figure 1). The city covers an area of 6 587.02 km², with 11 municipalities under its jurisdiction and a permanent population of 9.31 million. Nanjing has a subtropical monsoon climate with an average annual rainfall of 1 106 mm. Nanjing has four distinctive seasons (i.e. spring, summer, autumn and winter), with the temperature above 30 °C in summer and 2 - 10 °C in winter. Nanjing had grown rapidly during the past 30 years. Land subsidence occurred in different regions of Nanjing. In this paper, InSAR methodology with SAR images acquired from the Sentinel-1 between 2014 and 2019 has been used to characterize subsidence in Nanjing. Four types of buildings, including sluice (i.e. Qinhuai new river sluice), bridge (i.e. Shuiximen bridge), historic building (i.e. Sun Yat-sen's Mausoleum) and high-rise building (i.e. Greenland Square Zifeng Tower), are selected as monitoring cases and their locations are shown in Figure 1.

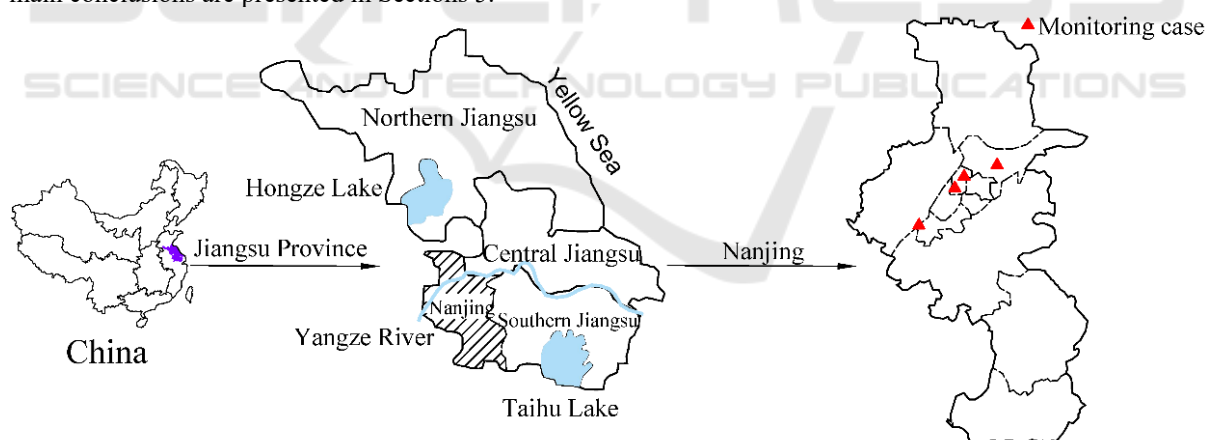


Figure 1: Location of Nanjing.

The European Space Agency (ESA) Sentinel-1 is a day-and-night, all-weather, polar-orbiting radar imaging mission for global monitoring of environment and security services at C-band. The Sentinel-1A and B are the two satellites that composes the Sentinel-1 radar mission, and were launched in April 2014 and April 2016, respectively. The Sentinel-1 SAR instrument can acquire data in four exclusive modes, namely Strip map (SM),

Interferometric Wide swath (IW), Extra Wide swath (EW) and Wave (WV) modes. Table 1 shows the selected 72 C-band VV-polarization ascending SAR images acquired by sentinel-1 in this study, covering the period October 8, 2014 to September 25, 2019.

Table 1: SAR data in monitoring area.

Parameter	Number
Satellite type; Date band; Spatial resolution	Sentinel-1; C-band (5.6 cm); 20 m
Up/down mode; Polarization mode; Side view	Ascending; VV; 39.92°
Acquisition time; Number of image	20141008-20190925; 72
Date level	SLC data (single view and multiple view)
Date of image	20141008, 20141102, 20141118, 20141220, 20150117 20150222, 20150306, 20150310, 20150322, 20150411 20150513, 20150614, 20150712, 20150716, 20150817 20150902, 20150918, 20151004, 20151016, 20151105 20151117, 20151207, 20151219, 20160108, 20160120 20160312, 20160328, 20160413, 20160429, 20160515 20160531, 20160616, 20160702, 20160714, 20160730 20160904, 20161002, 20161107, 20161209, 20170207 20170227, 20170416, 20170518, 20170603, 20170721 20170822, 20170919, 20171005, 20171110, 20171212 20180113, 20180214, 20180314, 20180403, 20180419 20180517, 20180622, 20180708, 20180805, 20180910 20181012, 20181113, 20181211, 20190112, 20190213 20190305, 20190418, 20190520, 20190621, 20190723 20190823, 20190925

3 RESEARCH METHOD

The Permanent Scatterers Synthetic Aperture Radar Interferometry (PSInSAR) is a InSAR technique. Compared with Differential Interferometric Synthetic Aperture Radar (DInSAR), it can overcome the influence of spatio-temporal coherence and atmospheric delay on SAR radar accuracy, and aims at ground deformation mapping with millimetric precision. Therefore, this paper adopts PSInSAR technology. The basic flow of PSInSAR data processing is shown in Figure 2.

PSInSAR identifies coherent radar targets (PS points) to monitor ground deformation. Hooper et al. (2004) proposed the identification algorithm of PS based on phase characteristics, which includes registration, radiometric calibration, PS detection and interference processing for single-view complex SAR images. After that, the differential interference phase set of each PS point in each differential interferogram can be obtained.

The phase residual of the PS point x in the scene i interferogram is shown as follows:

$$\varphi_{x,i} = \varphi_{def,x,i} + \varphi_{a,x,i} + \varphi_{orb,x,i} + \varphi_{\epsilon,x,i} + n_{x,i} \quad (1)$$

where $\varphi_{x,i}$ is the phase value of the pixel x of the

scene i interferogram, $\varphi_{def,x,i}$ is the deformation phase in radar line of sight direction, $\varphi_{a,x,i}$ is the delay phase difference of satellite transit atmosphere at different times, $\varphi_{orb,x,i}$ is the phase due to error in the DEM, $\varphi_{\epsilon,x,i}$ is the DEM error phase, $n_{x,i}$ is the phase of noise.

If φ_{def} , φ_a and φ_{orb} are spatially correlated over distances of a specified length scale L , and that φ_{ϵ} and n are uncorrelated over the same distance, with the mean of Zero. Then, the mean value of each phase in the circular region with pixel x as the center of the circle and pixel L as the radius can be expressed as:

$$\bar{\varphi}_{x,i} = \bar{\varphi}_{def,x,i} + \bar{\varphi}_{a,x,i} + \bar{\varphi}_{orb,x,i} \quad (2)$$

Subtracting formula (2) from formula (1) leads to:

$$\varphi_{x,i} - \bar{\varphi}_{x,i} = \varphi_{\epsilon,x,i} + n_{x,i} - \bar{n}'_{x,i} \quad (3)$$

where $\bar{n}' = (\bar{\varphi}_{def} - \varphi_{def}) + (\bar{\varphi}_a - \varphi_a) + (\bar{\varphi}_{orb} - \varphi_{orb})$.

The DEM error phase $\varphi_{\epsilon,x,i}$ and the vertical

baseline $B_{\perp,x,i}$ are proportional to each other, the formula (3) also can be represented as follows:

$$\varphi_{x,i} - \bar{\varphi}_{x,i} = B_{\perp,x,i}K_{\epsilon,x} + n_{x,i} - \bar{n}'_{x,i} \quad (4)$$

where $K_{\epsilon,x}$ is a proportionality constant.

Then, in all available interferogram, the smallest square method is used to estimate $K_{\epsilon,x}$:

$$\gamma_x = (1/N) | \sum_{i=1}^N \exp\{j(\varphi_{x,i} - \bar{\varphi}_{x,i} - \hat{\varphi}_{\epsilon,x,i})\} | \quad (5)$$

where, γ_x is a measure of the temporal coherence based on pixel x , N is the number of available interference patterns and $\hat{\varphi}_{\epsilon,x,i}$ is our estimate of $\varphi_{\epsilon,x,i}$.

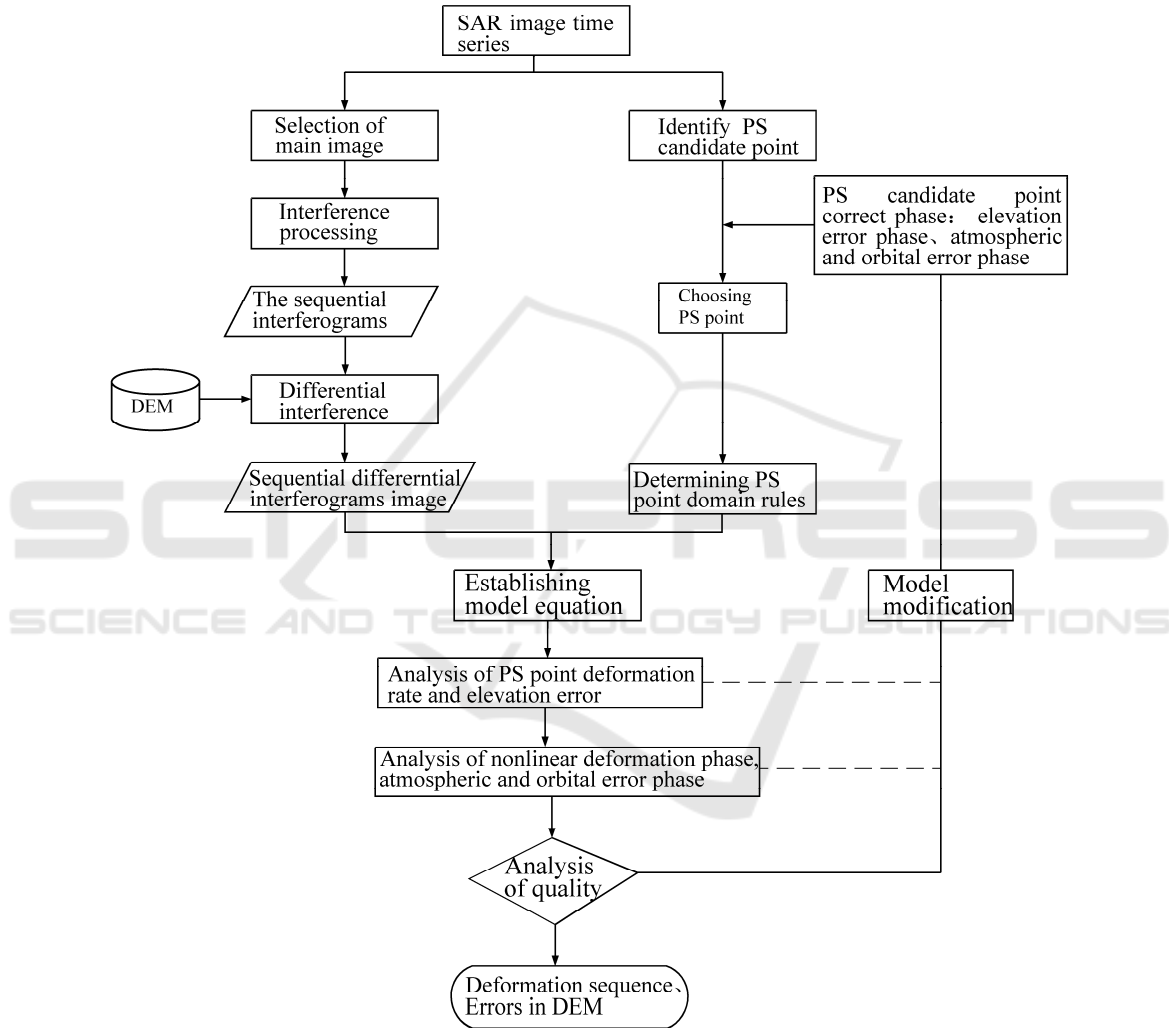


Figure 2: The basic flow chart of PSInSAR data processing.

4 RESULTS

In this paper, 72 radar interference images in Nanjing city from October 8, 2014 to September 25, 2019 had been obtained to analyze the deformations of the selected sluice, bridge, historical building and

high-rise building. Figure 3 shows the uplift or settlement deformations of PS points in study area. The results indicate that the annual average ground motion velocity (mm/yr) was mainly in the range of -18 mm/yr to 18 mm/yr.

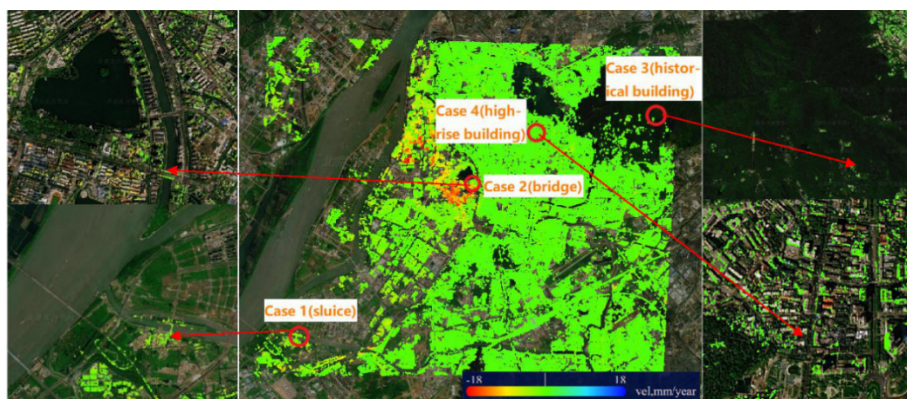


Figure 3: Map of ground deformation in study area.

Figure 4 and Table 2 shows four deformation record examples (i.e. Qinhuai new river sluice, Shuiximen bridge, Sun Yat-sen's Mausoleum and Greenland Square Zifeng Tower). The negative value in the picture represents settlement and positive value represents uplift. It can be seen from the picture that in the past 5 years, (i) The annual average motion velocity of the sluice, bridge, historic building and high-rise building range from

-3.3 mm/yr to -0.5 mm/yr, -0.1 mm/yr to 1.3 mm/yr, -0.6 mm/yr to 1.0 mm/yr and -0.2 mm/yr to 1.0 mm/yr, respectively, (ii) The most of the cases were relatively stable within a limited deformation range, and their cumulative deformation is -4.4 mm, -8.3 mm, -3.7 mm and 2.6 mm respectively, (iii) Their average deformation is -2.4 mm, -4.6 mm, 1.1 mm and 1.3 mm respectively, so the two buildings are in the more stable state than the rests.

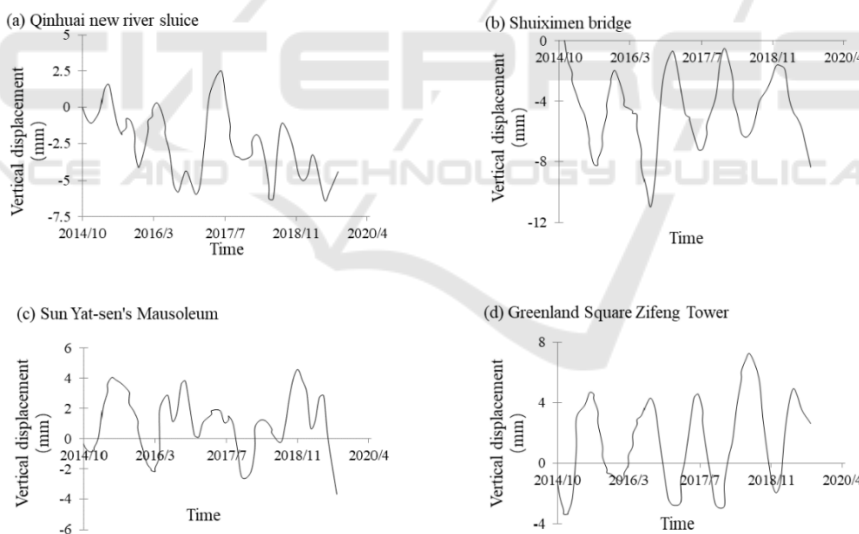


Figure 4: Four deformation record examples: (a) Qinhuai new river sluice, (b) Shuiximen bridge, (c) Sun Yat-sen's Mausoleum, (d) Greenland Square Zifeng Tower.

Table 2: The deformation data of four cases.

Cases	The annual average motion velocity(mm/yr)		The cumulative deformation(mm)	The average deformation(mm)
	min	max		
Case 1	-3.3	-0.5	-4.4	-2.4
Case 2	-0.1	1.3	-8.3	-4.6
Case 3	-0.6	1.0	-3.7	1.1
Case 4	-0.2	1.0	2.6	1.3

5 CONCLUSIONS

In this paper, the Qinhuai new river sluice, Shuiximen bridge, Sun Yat-sen's Mausoleum, and Greenland Square Zifeng Tower in Nanjing are selected as study cases. SAR images acquired by sentinel-1 and PSInSAR technology have been used to characterize subsidence in Nanjing. The main conclusions are as follows:

1) In the past 5 years, most of the study area was relatively stable within a limited deformation range. In all cases, the maximum annual average settlement velocity and uplift velocity were 3.3 mm/yr and 1.3 mm/yr respectively, the maximum cumulative settlement and uplift were only 8.3 mm and 2.6 mm respectively, and the maximum average settlement and uplift were only 4.6 mm and 1.3 mm respectively. Qinhuai new river sluice and Shuiximen bridge existed a slight settlement trend, while Sun Yat-sen's Mausoleum and Greenland Square Zifeng Tower tended to be a stable state with small scale fluctuation.

2) Due to the lack of leveling results from the above four cases, the PSInSAR technology proposed by Hooper et al. (2004) has not been verified in this study. The distribution of PS points is related to the objects (e.g. roofs, road surfaces, rocks, etc) and landforms of the research area, and the position of PS point is random. Therefore, the manually arranged leveling point and the PS point identified by PSInSAR technology are unlikely to be in the same position. How to compare the displacement results of PS points and leveling points to verify the reliability of PSInSAR in this study is worthy of further research.

3) Some factors such as soft soil layer with high compressibility and low bearing capacity, falling groundwater levels, and surcharge loads (e.g. high-rise buildings, subways) can result in urban land subsidence in Nanjing city. The results showed there was no obvious uplift trend and settlement trend for most of the study area. The reasons for the land uplift in some areas may be related to stress release of foundation soil, the rise of groundwater level and the decrease of load. But the real reason needs to be further studied.

4) PSInSAR technique can provide millimeter-level accuracy in urban land subsidence monitoring without much time and high cost, and it is worthy of further discussion in other deformation research work based on PSInSAR technology.

ACKNOWLEDGMENTS

This work was supported by the Water Resources Science and Technology Project of Jiangsu Province (Grant No. 2019022), and the Science and Technology Project of Jiangsu Province (Grant No. BM2018028).

REFERENCES

- Alani, A. M., Tosti, F., & Ciampoli, L. B. (2020). An integrated investigative approach in health monitoring of masonry arch bridges using GPR and InSAR technologies. *NDT and E International*, *115*, 102-288.
- Baer, G., Schattner, U., & Wachs, D. (2002). The lowest place on Earth is subsiding-An InSAR (interferometric synthetic aperture radar) perspective. *Geological Society of America Bulletin*, *114*, 12-23
- Fobert, M. A., Singhroy, V., & Spray, J. G. (2021). InSAR Monitoring of Landslide Activity in Dominica. *Remote Sens*, *13*, 8-15.
- Guo, R., Li, S., & Chen, Y. (2021). Identification and monitoring landslides in Longitudinal Range-Gorge Region with InSAR fusion integrated visibility analysis. *Landslides*, *18*, 551-568.
- Hooper, A., Zebker, H., & Segall, P. (2004). A new method for measuring deformation on volcanoes and other natural terrains using InSAR persistent scatterers. *Geophysical Research Letters*, *31*, 1-5.
- Hooper, A. (2008). A multi-temporal InSAR method incorporating both persistent scatterer and small baseline approaches. *Geophysical Research Letters*, *35*, 96-106.
- Koning, M. D., Haasnoot, J. K., & Buuren, R. V. (2020). Determination of amount of land subsidence based on INSAR and LiDAR monitoring for a dike strengthening project. *Plahs*, *382*, 57-62.
- Liang, H., Li, X., & Chen, R. (2021). Mapping Surface Deformation Over Tatun Volcano Group, Northern Taiwan Using Multitemporal InSAR. *IEEE Journal of Selected Topics in Applied Earth Observations and Remote Sensing*, *14*, 2087-2095.
- Pritchard, M. E. & Simons, M. (2013). An InSAR-based survey of volcanic deformation in the central Andes. *Geochemistry Geophysics Geosystems*, *05*, 1-42.
- Rivera, A. M. & Amelung, F. & Mothes, P. (2017). Ground deformation before the 2015 eruptions of cotopaxi volcano detected by insar. *Geophysical Research Letters*, *44*, 6607-6615.
- Smith, R., & Knight, R. (2019). Modeling Land Subsidence Using InSAR and Airborne Electromagnetic Data. *Water Resources Research*, *13*, 2801-2819.
- Wright, T. J., Parsons, B., & England, P. C. (2004). InSAR Observations of Low Slip Rates on the Major Faults of Western Tibet. *Science*, *305*, 236-239.

- Xu, Z., Cheng, T., & Hong, S. (2018). Review on applications of remote sensing in urban flood modeling. *Kexue Tongbao, Chinese Science Bulletin*, 63, 2156-2166.
- Yan, S., Ruan, Z., & Liu, G. (2016). Deriving Ice Motion Patterns in Mountainous Regions by Integrating the Intensity-Based Pixel-Tracking and Phase-Based D-InSAR and MAI Approaches: A Case Study of the Chongce Glacier. *Remote Sensing*, 8, 6-11.
- Yang, Z. F., Li, Z. W., & Zhu, J. J. (2020). Use of SAR/InSAR in Mining Deformation Monitoring, Parameter Inversion, and Forward Predictions: A Review. *IEEE Geoscience and Remote Sensing Magazine*, 8, 71-90.
- Yu, H. W., Xing, M. D., & Yuan, Z. H. (2021). Baseline Design for Multibaseline InSAR System: A Review. *Miniaturization for Air and Space Systems*, 02, 17-24.
- Zhou, D., Simic-Milas, A., & Yu, J. (2020). Integrating RELAX with PS-InSAR Technique to Improve Identification of Persistent Scatterers for Land Subsidence Monitoring. *Remote Sensing*, 12, 27-30.

